https://doi.org/10.48048/tis.2024.7779

The Potential of Sodium Silicate from Rice Husk as Corrosion Inhibitor on Mild Steel

Atiek Rostika Noviyanti[1,*], Solihudin[1], Haryono[1], Yudha P. Budiman[1], Agus Solehudin[2] and Muhamad Diki Permana[3,4]

[1]Department of Chemistry, Faculty Mathematics and Natural Sciences, Universitas Padjadjaran Sumedang, West Java 45363, Indonesia
[2]Department of Mechanical Engineering Education, Faculty of Technology and Vocational Education, Universitas Pendidikan Indonesia, West Java 40154, Indonesia
[3]Integrated Graduate School of Medicine, Engineering and Agricultural Sciences, University of Yamanashi, Kofu 4008511, Japan
[4]Center for Crystal Science and Technology, University of Yamanashi, Kofu 4008511, Japan

([*]Corresponding author's e-mail: atiek.noviyanti@unpad.ac.id)

Received: 29 November 2023, Revised: 24 December 2023, Accepted: 31 December 2023, Published: 10 May 2024

Abstract

Study of sodium silicate from rice husks as coating material is reported. The extraction was conducted *via* precipitation method with sodium hydroxide, nitric acid and ethanol at pH 8. The resulting silica was tested as hydrophobic coating by coating it on a glass surface. Based on the value of the contact angle, silica has good hydrophobic properties. The highest hydrophobic properties were obtained from sample, which labeled as Si10A:Si5B with an average contact angle of 105.3 °. Investigation of the potential application of sodium silicate as an inhibitor of corrosion has been conducted by coating it on steel surfaces. The effect of the concentration of sodium silicate was conducted at 0, 10, 20 and 30 ppm and found that the morphology of steel coated with 20 ppm has the lowest corrosion rate with 81 % inhibition efficiency.

Keywords: Hydrophobic, Sodium silicate, Rice husk, Contact angle, Corrosion inhibitor

Introduction

Research on hydrophobic coating materials has always attracted attention due to their wide application in ultra-dry surfaces. The degree of hydrophobicity of a coating is determined by its composition and morphology [1-3]. Silica is one of the hydrophobic coating materials with non-polar properties [4]. Silica can be produced via chemical synthesis processes using tetraethoxysilane (TEOS), or tetramethoxysilane (TMOS) substrates [5,6]. However, TEOS and TMOS are relatively expensive and toxic. Thus, getting a new silica source that is cheap and has nontoxic properties is the solution to this problem.

Silica (SiO_2) is one of the most abundant compounds on the earth's crust and is found in crystalline and non-crystalline (amorphous) forms. Crystalline silica has advantages such as high stability, being insoluble in water, and being active on the surface when reactive oxygen is released [7]. Moreover, silica is the most studied material due to its hybrid structure, resistance to high temperatures, high flexibility, high gas permeability and low surface energy. Even nanosized silica has strength and is abrasion-resistant, aging and climate. Therefore, silica-nano is widely used in heat insulators, bioactive supports, paints, plastics, rubber, coatings, drug delivery systems and composite materials [8,9].

Rice husk ash is waste that is no longer used which is the result of burning the husks. Rice husk ash contains almost 95 % silica [10]. Based on 2019 Food and Agriculture Organization (FAO) data, Indonesia is ranked 3rd highest after China and India, with around 54.60 million tons of rice production [11]. However, the use of rice husks is still lacking. Processing rice husk waste into economically valuable material products should be carried out using an environmentally friendly industrial process approach. Silica extraction from rice husks without burning, in this case with a simple precipitation method, is desired because it is environmentally friendly and has a relatively low cost. The extraction of silica by combustion will produce air pollution, resulting in health issues, especially respiratory problems [12-14].

Amorphous silica has an arrangement of atoms and molecules in random and irregular patterns. Because of this, amorphous silica has a complicated spherical structure. This complex structure causes a high surface area, usually above 3 m^2/g [15,16]. Amorphous silica can be made in various forms such as

sol of silica, silica gels, precipitated silica and pyrogenic silicas [17]. Amorphous silica has been classified as a nontoxic material and does not cause silicosis, whereas crystalline silica is very toxic. However, if the amorphous silica in air (maximum concentration in the range of 2 mg/m^3) is inhaled for 8 h continuously, it will impact respiratory health [18]. Under various conditions, amorphous silica is considered to be more reactive than crystalline silica. The level of reactivity of amorphous silica is due to a hydroxyl or silanol group obtained after heating to a temperature of 400 °C. The silanol group (–SiOH) is present on the silica surface, which causes its reactive side [19]. This active side of silica also causes it to bond strongly to the surface of a metal. Therefore, silica can be a corrosion inhibitor material [20].

In this research, silica was extracted from rice husk ash, and made into sodium silicate as a hydrophobic surface to obtain anti-corrosion properties. Although several reports have been reported regarding the use of silica from rice husk ash, its application as a corrosion inhibitor has never been carried out [21-23]. Therefore, in this study, we report the potential application of silica from rice husks as a hydrophobic coating and corrosion inhibitor on mild steel.

Materials and methods

Materials

The materials used in this research were rice husks supplied by the Sumedang Region (Indonesia) and mild steel test objects (1.9×1.5×0.8 cm^3). The chemical reagent was purchased from Sigma Aldrich (St. Louis, MO, USA), including hydrochloric acid (HCl, 37 %), sodium hydroxide (NaOH, 99 %), ethanol (C_2H_5OH, 96 %), acetone (C_3H_6O, 99.5 %) and nitric acid (HNO_3, 68 %).

Extraction of silica from rice husk

Rice husks were cleaned by soaking with distilled water for 24 h followed by drying at 90 °C for 24 h. Afterwards, the rice husks were soaked in 1 N HCl solution at 75 °C for 1 h to remove metal oxide impurities. The rice husks were then washed several times with distilled water and then dried at 90 °C for 24 h. Afterwards, the silica was extracted by immersing 20 g of rice husk in 300 mL NaOH and heated at 90 °C in water bath for 1 h. The solid was then filtered, then dissolved in ethanol and HNO_3 with different concentrations of 3 N and 4 N until it reached a pH of 8 while stirring for 45 min. The mixture was then treated with centrifugation at 4,000 rpm for 5 min. The obtained silica gel was then washed with an aqueous solution, then separated by centrifugation at 4,000 rpm for 5 min. This process is repeated until a white silica gel is obtained. Silica gel was calcined at 600 °C for 1 h to get solid silica powder. Then, the silica powder was characterized by X-ray diffraction (XRD, PANalytical X'Pert Pro, PW 3040/x0) using Cu Kα radiation (λ = 0.1542 nm) at room temperature.

Hydrophobic properties of silica

Testing the hydrophobic properties of silica on mild steel plates was carried out by coating colloidal silica on the glass surface. Colloidal silica is made by dissolving sodium silicate in a solution of nitric acid and ethanol (pH 8) and then rotated with 2 different rotational speeds, namely, 1,000 rpm (SiA) and 2,000 rpm (SiB) for 5 min. The silica gel formed was washed with distilled water.

The determination of the contact angle of a liquid droplet on a surface generally uses the approach that the droplet is circular (or part of a circle). The calculation of contact angles can be approached by applying Eqs. (1) and (2), respectively, for contact angles less than 90 ° and between 90 to 180 ° (**Figure 1**) [24,25].

The 2 colloids were mixed with various wt% of SiA and SiB, as shown in **Table 1**. Ethanol was added and then mixed by ultrasonication (20 kHz) for 30 min. The glass was immersed in H_2SO_4 and H_2O_2 (50:50) for 6 h, and shaken for 30 min under ultrasonication, then rinsed with acetone and distilled water. Glass coating with colloidal silica was successively conducted by immersed for 15 min, then drying and heating it at 250 °C for 2 h.

$$\theta = 2\ arctan\ (2\ h/l) \quad (1)$$

$$\theta = 90\ ° + arccos\ [(4\ hl)\ /\ (4\ h^2 + l^2)] \quad (2)$$

Table 1 Colloid composition of silica for coating.

Sample name	SiA (g)	SiB (g)	Ethanol (g)
5SiA	5	0	95
5SiB	0	5	95
5SiA:10SiB	5	10	85
10SiA:5SiB	10	5	85

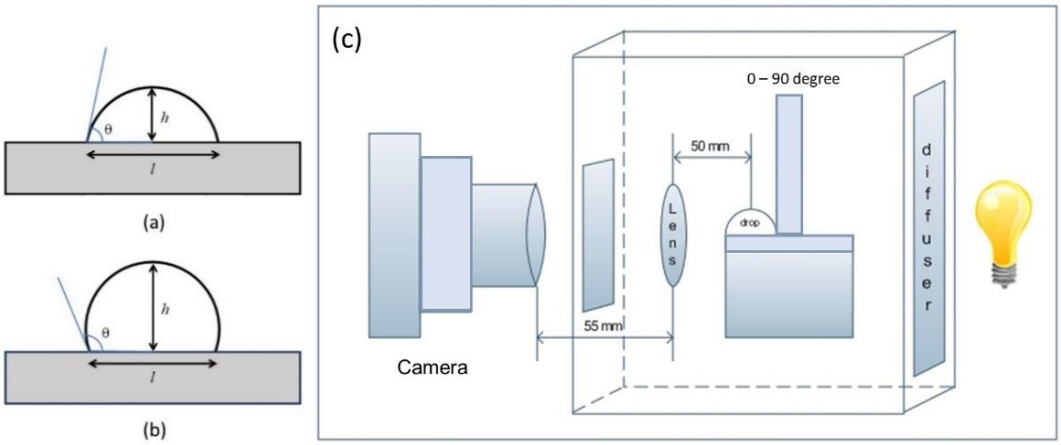

Figure 1 Illustration of droplets with (a) hydrophilic (θ < 90 °), (b) hydrophobic (90 ° > θ > 180 °), and (c) schematic of the contact angle measurement tool.

Silica corrosion inhibition test

Sodium silicate solutions were made by dissolving silica with various concentrations of 10, 20 and 30 ppm in a 3 M NaOH solution [26]. The corrosion rate (*R*, mmpy) is determined using Eq. (3), where *W* is loss weight (mg), *A* is area of the specimen (cm^2), *t* is time (h) and *D* is density of the specimen (g/m^3).

$$R = (87.6 \times W)/(A \times t \times D) \quad (3)$$

A silica corrosion inhibition test was carried out on mild steel specimens measuring 1.9×1.5×0.8 cm^3, which had been cleaned with sandpaper, then washed with distilled water, smeared with acetone, and dried with an air stream. Steel specimens were weighed and then immersed in distilled water and nano-silica solution as an inhibitor solution at room temperature for 12 days. After soaking, the specimens were cleaned with a brush in distilled water to calculate the percentage of inhibition efficiency (IE) from the corrosion rate data using Eq. (4) [27], where R_o is corrosion rate without the addition of an inhibitor (mmpy) and R_I is corrosion rate with the addition of an inhibitor (mmpy)

$$\text{Inhibitor Efficiency} = ((R_0 - R_1)/R_0) \times 100\ \% \quad (4)$$

Results and discussion

Extraction of silica from rice husk

When extracting silica from rice husk ash, silica will be reacted in a basic NaOH solution to form sodium silicate. This sodium silicate can then be separated from the other components in the husk ash. After that, sodium silicate turns back into silica in gel form by reducing the pH using HNO_3. The reaction that occurs is written in Eqs. (5) and (6).

$$SiO_{2\,(s)} + 2NaOH_{\,(aq)} \rightarrow Na_2SiO_{3\,(aq)} + H_2O_{\,(l)} \quad (5)$$

$$Na_2SiO_{3\,(aq)} + 2HNO_{3\,(aq)} \rightarrow SiO_{2\,(s)} + 2NaNO_{3\,(s)} + H_2O_{\,(l)} \quad (6)$$

The high electronegativity of the oxygen makes Si atom more electropositive and an unstable intermediate [SiO_2OH] is formed. Next occurs dehydrogenation and the 2nd hydroxyl ion will bind with hydrogen to release water molecules. Two Na^+ ions will balance the negative charge formed and interact with SiO_3^{2-} ions to form sodium silicate (Na_2SiO_3). The resulting sodium silicate (Na_2SiO_3) solution was added with nitric acid and ethanol until the pH of the solution was 8 while stirring with a magnetic stirrer to extract the silica precipitate. The mechanism of formation of sodium silicate and image of colloidal silica and silica powder calcined at 600 °C are shown in **Figure 2**.

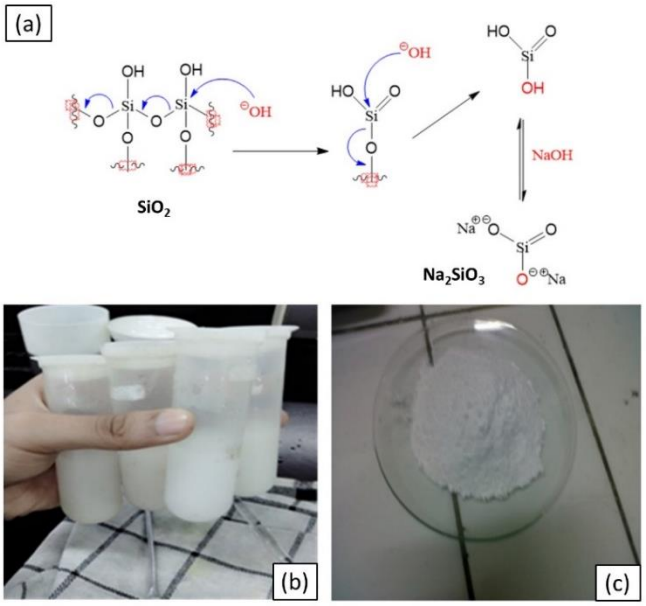

Figure 2 (a) the reaction mechanism for the formation of sodium silicate, (b) colloidal silica, and (c) silica powder after calcined at 600 °C.

The XRD pattern of silica is shown in **Figure 3**. Pretreatment of rice husk with HNO_3 produces white amorphous silica with high purity [28]. The XRD pattern shows that the silica produced was an amorphous form, with a typical broad peak at 2θ = 21 - 22 ° for both prepared with 3 and 4 N HNO_3 concentrations [29,30]. This means that the various addition of HNO_3 concentrations did not affect the differences in silica structure. Besides that, there were no other peaks detected in the XRD pattern, indicating the purity of the silica produced [31].

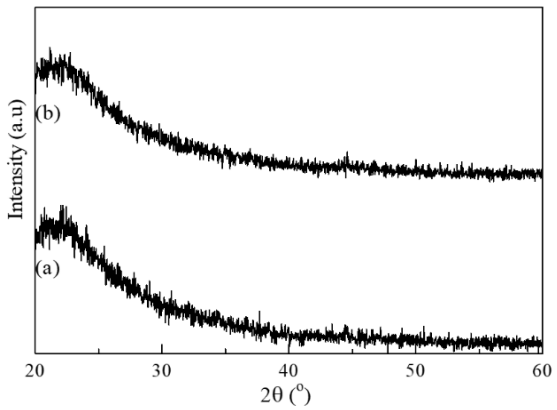

Figure 3 XRD pattern of amorphous silica, prepared with (a) 3 and (b) 4 N HNO_3 concentrations.

Hydrophobic properties of silica

The hydrophobic properties of silica are tested by measuring the contact angle. In this study, the contact angle was tested by dropping 30 µL of distilled water on a glass surface that had been coated with silica. **Table 2** and **Figure 4** shows the contact angle results of various samples. The contact angle of 5SiB

is greater than 5SiA, indicating that the rotation speed has an impact on the formation of the nano-silica structure, but the effect on filling between the 2 does not give a comparable effect. The average contact angle of sample 10A:5B is 105.3 ± 1.1 °, which means it shows hydrophobic properties. 10A:5B has hydrophobic properties thought to be due to the reduction of hydroxyl groups compared to other samples [32]. The use of silica acid sol which has hydroxyl groups, through condensation and hydrolysis reactions forms siloxane crosslinks which reduce the number of hydroxyls [33,34].

Table 2 Contact angle of silica.

Sample	Contact angle (°)			Average (°) ± standard deviation
	1	2	3	
5SiA	70	74	72	72.0 ± 2.0
5SiB	82	84	84	83.3 ± 1.1
5SiA:10SiB	70	70	70	70.0 ± 0.0
10SiA:5SiB	106	106	104	105.3 ± 1.1

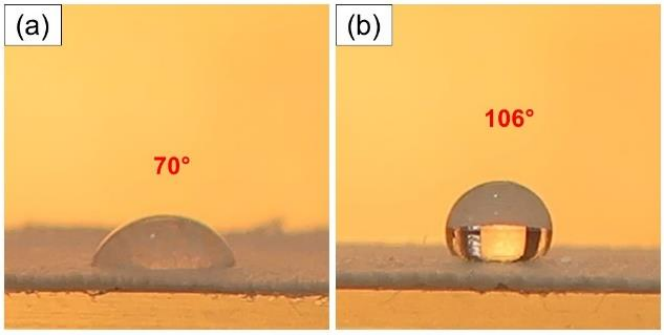

Figure 4 Contact angle measurement on (a) Si5A and (b) Si10A:Si5B.

In addition, this hydrophobicity also increases the nanoscale secondary roughness on the substrate surface [35]. **Figure 5** shows scanning electron microscope (SEM) images of each silica sample. In addition, surface roughness visualization was used using Image Processing and Analysis in Java (ImageJ). Ra, which is the absolute average relative to the length of the base, is used to determine the roughness value. **Figure 5(d)** shows that sample 10A:5B has the highest roughness due to the presence of nanocavities on the surface resulting in a hydrophobic layer [36]. This is different from other samples which are more homogeneous. The Ra values for Si5A, Si5B, Si5A:Si10B and Si10A:Si5B are 41.5, 44.8, 41.2 and 47.8, respectively. This value is in agreement with the contact angle value obtained.

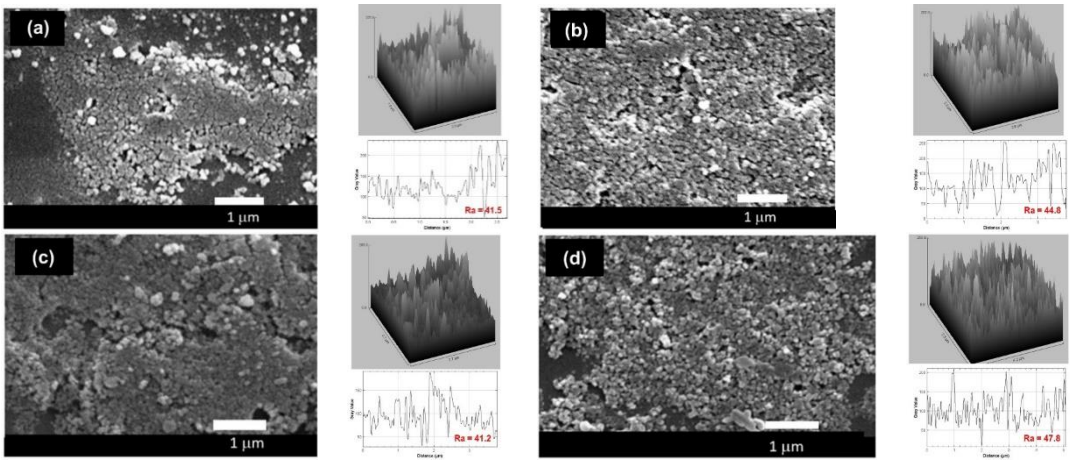

Figure 5 SEM image of (a) Si5A, (b) Si5B, (c) Si5A:Si10B, and (d) Si10A:Si5B.

Determination of corrosion rate

The effect of sodium silicate concentration on the corrosion rate of steel was observed at 10, 20 and 30 ppm. The effect of sodium silicate concentration on corrosion rate and inhibition efficiency is shown in **Table 3** and **Figure 6**. Sodium silicate coating has been proven to inhibit corrosion growth. Ten ppm sodium silicate has an inhibition efficiency of up to 69.70 %. Increasing the sodium silicate concentration up to 20 ppm could reduce the corrosion rate significantly, but the corrosion rate was almost unchanged by increasing the concentration up to 30 ppm. Silica, especially in the form of free silanol, can chemically bond with the steel surface to produce Fe-O-Si chemical bonds. The coated sodium silicate undergoes hydrolysis and polymerization reactions that occur simultaneously. The Si-O-Na groups of sodium silicate polymerize in solution to form Si-O-Si bonds. In addition, the Si-O-H group from the precursor undergoes hydrolysis with the hydroxyl group in mild steel (Fe-O-H). Finally, the curing stage allows the formation of Fe-O-Si covalent bonds, namely metallo-siloxane bonds [37].

Table 3 Effect of sodium silicate concentration on the corrosion rate and inhibition efficiency.

Silica (ppm)	Lost weight (mg)	Corrosion rate (mmpy)	Inhibitor efficiency (%)
0	0.1571	0.5804	-
10	0.0467	0.1758	69.70
20	0.0284	0.1049	81.90
30	0.0285	0.1052	81.80

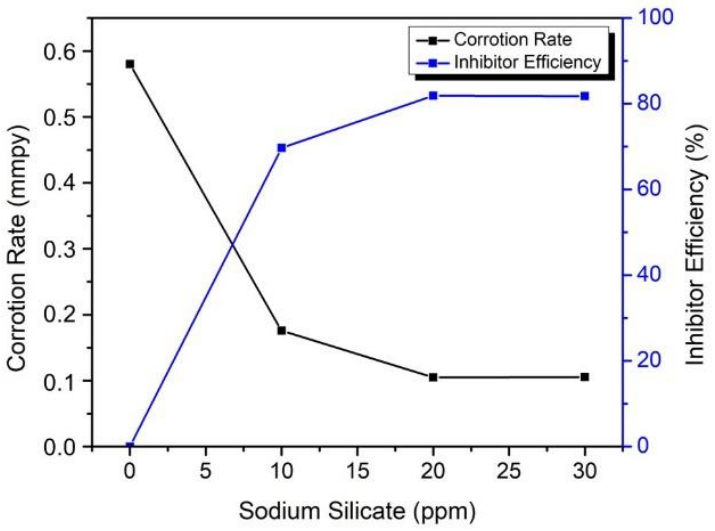

Figure 6 Effect of sodium silicate on the corrosion rate and inhibitor efficiency of steel.

Figure 7 shows the SEM image of mild steel after 12 days. In **Figure 7(a)**, without the addition of silica, the surface morphology of the steel shows corrosion which is characterized by an inhomogeneous surface. For the addition of 10 ppm silica (**Figure 7(b)**), only slightly lower corrosion products were shown with increased homogeneity, only on the uneven surface areas. The addition of 20 and 30 ppm silica showed a homogeneous surface, and almost no corrosion products were visible on the steel surface (**Figures 7(c) - 7(d)**). Increasing the sodium silicate concentration causes the formation of a thicker film, this explains the better corrosion properties of the prepared sodium silicate-coated mild steel [38]. However, at a sodium silicate concentration of 30 ppm, the coating resistance was lower than 20 ppm. The decrease in coating resistance is caused by the penetration of water and corrosive ionic species into the coating, thereby increasing the conductivity of the coating. Thus, coatings that exhibit lower coating resistance should have higher coating porosity compared to coatings at 20 ppm that offer optimal coating characteristics [37]. Apart from that, the effect of decreasing the effectiveness of corrosion inhibitors is also believed to be due to competition and repulsion between sodium silicate molecules as a corrosion inhibitor.

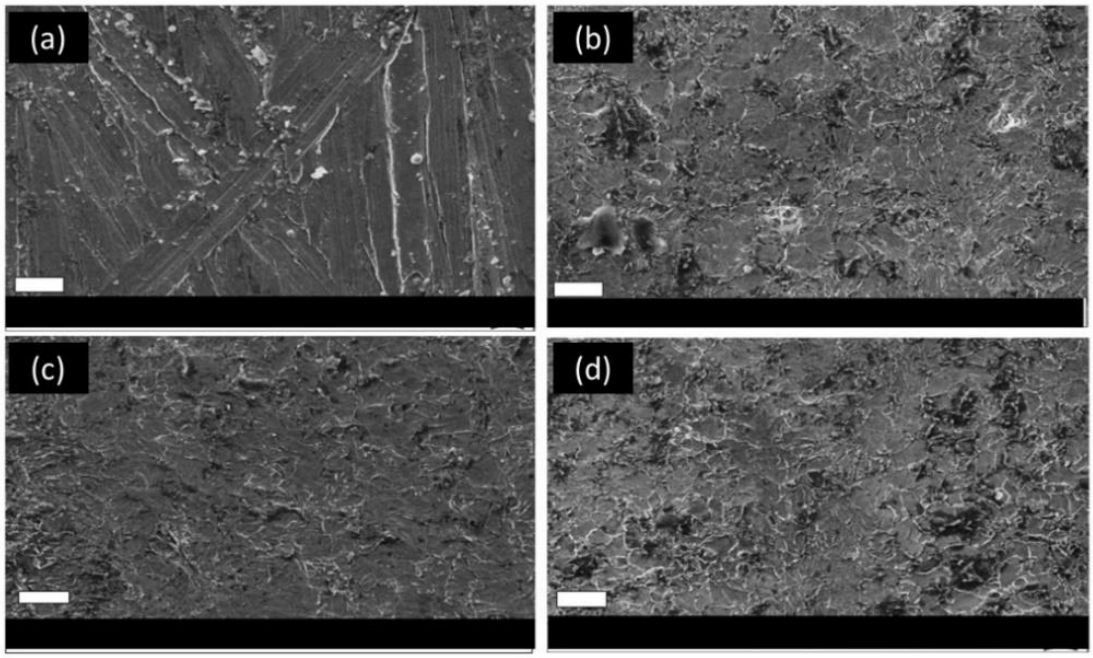

Figure 7 Effect of sodium silicate inhibitor concentration on the surface morphology of (a) 0 ppm, (b) 10 ppm, (c) 20 ppm, and (d) 30 ppm on mild steel after 12 days; the scale shows a length of 20 µm.

Conclusions

The amorphous phase of silica was successfully synthesized from rice husk using the precipitation method. Extracted silica can be a hydrophobic coating agent. The greatest hydrophobic properties were obtained from sample 10A:5B with an average contact angle of 105.3 °. Other sample compositions show a low contact angle value, which means that the shaking speed of colloid production affects the quality of the silica coating. Sodium silicate prepared from extracted silica has the potential as a corrosion inhibitor because it can reduce the corrosion rate and increase the efficiency of inhibition. The highest inhibition efficiency was obtained at a concentration of 20 ppm of sodium silicate, which was 81.9 %.

Acknowledgements

The authors are grateful to Universitas Padjadjaran, Indonesia, who has funded this work under Academic Leadership Grant (ALG) through project number 1549/UN6.3.1/PT.00.2023, 27 March 2023.

References

[1] K Jeevajothi, RT Subasri and KRCS Raju. Transparent, non-fluorinated, hydrophobic silica coatings with improved mechanical properties. *Ceram. Int.* 2013; **39**, 2111-6.
[2] W Pramualkijja and N Jiratumnukul. Physical properties and morphology of siloxane-polyacrylate dispersion and coating films. *J. Coating. Tech. Res.* 2020; **17**, 1277-88.
[3] IS Bayer. Superhydrophobic coatings from ecofriendly materials and processes: A review. *Adv. Mater. Interface* 2020; **7**, 2000095.
[4] F Chi, D Liu, H Wu and J Lei. Mechanically robust and self-cleaning antireflection coatings from nanoscale binding of hydrophobic silica nanoparticles. *Sol. Energ. Mater. Sol. Cell.* 2019; **200**, 109939.
[5] KD Kim and HT Kim. Formation of silica nanoparticles by hydrolysis of TEOS using a mixed semi-batch/batch method. *J. Sol Gel Sci. Tech.* 2002; **25**, 183-9.
[6] H Kaur, S Chaudhary, H Kaur, M Chaudhary and KC Jena. Hydrolysis and condensation of tetraethyl orthosilicate at the air-aqueous interface: Implications for silica nanoparticle formation. *ACS Appl. Nano Mater.* 2022; **5**, 411-22.

[7] E Monfort, A Mezquita, E Vaquer, I Celades, V Sanfelix and A Escrig. Ceramic manufacturing processes: Energy, environmental, and occupational health issues. *Compr. Mater. Process.* 2014; **8**, 71-102.
[8] M Yazdimamaghani, T Pourvala, E Motamedi, B Fathi, D Vashaee and L Tayebi. Synthesis and characterization of encapsulated nanosilica particles with an acrylic copolymer by *in situ* emulsion polymerization using thermoresponsive nonionic surfactant. *Materials* 2013; **6**, 3727-41.
[9] IA Sharaky, FA Megahed, MH Seleem and AM Badawy. The influence of silica fume, nano silica and mixing method on the strength and durability of concrete. *SN Appl. Sci.* 2019; **1**, 575.
[10] B Singh. *Rice husk ash*. Woodhead Publishing, Cambridge, 2018, p. 417-60.
[11] N Bandumula. Rice production in Asia: Key to global food security. *Proc. Natl. Acad. Sci. India Biol. Sci.* 2018; **88**, 1323-8.
[12] HB Dizaji, T Zeng, I Hartmann, D Enke, T Schliermann, V Lenz and M Bidabadi. Generation of high quality biogenic silica by combustion of rice husk and rice straw combined with pre- and post-treatment strategies-A review. *Appl. Sci.* 2019; **9**, 1083.
[13] M Noushad, IA Rahman, A Husein, D Mohamad and AR Ismail. A simple method of obtaining spherical nanosilica from rice husk. *Int. J. Adv. Sci. Eng. Inform. Tech.* 2012; **2**, 28-30.
[14] R Rajan, Y Zakaria, S Shamsuddin and NFN Hassan. Robust synthesis of mono-dispersed spherical silica nanoparticle from rice husk for high-definition latent fingermark development. *Arabian J. Chem.* 2020; **13**, 8119-32.
[15] LT Zhuravlev. The surface chemistry of amorphous silica. Zhuravlev model. *Colloid. Surface. Physicochem. Eng. Aspect.* 2000; **173**, 1-38.
[16] J Schaller, A Cramer, A Carminati and M Zarebanadkouki. Biogenic amorphous silica as main driver for plant available water in soils. *Sci. Rep.* 2020; **10**, 2424.
[17] Y Jin, A Li, SG Hazelton, S Liang, CL John, PD Selid, DT Pierce and JX Zhao. Amorphous silica nanohybrids: Synthesis, properties and applications. *Coord. Chem. Rev.* 2009; **253**, 2998-3014.
[18] JG Croissant, KS Butler, JI Zink and CJ Brinker. Synthetic amorphous silica nanoparticles: Toxicity, biomedical and environmental implications. *Nat. Rev. Mater.* 2020; **5**, 886-909.
[19] M Ide, M El-Roz, ED Canck, A Vicente, T Planckaert, T Bogaerts, IV Driessche, F Lynen, VV Speybroeck, F Thybault-Starzyk and PVD Voort. Quantification of silanol sites for the most common mesoporous ordered silicas and organosilicas: Total *versus* accessible silanols. *Phys. Chem. Chem. Phys.* 2013; **15**, 642-50.
[20] M Rimoldi and A Mezzetti. Site isolated complexes of late transition metals grafted on silica: Challenges and chances for synthesis and catalysis. *Catal. Sci. Tech.* 2014; **4**, 2724-40.
[21] V Thangarasu and R Anand. *Comparative evaluation of corrosion behavior of Aegle Marmelos Correa diesel, biodiesel, and their blends on aluminum and mild steel metals*. *In*: AK Azad and M Rasul (Eds.). Advanced biofuels applications, technologies and environmental sustainability. Woodhead Publishing, Cambridge, 2019, p. 443-71.
[22] GN Marsh and C Chew. Well man clinic in general practice. *Br. Med. J.* 1984; **288**, 200-1.
[23] N Zulfareen, K Kannan, T Venugopal and S Gnanavel. Synthesis, characterization and corrosion inhibition efficiency of N-(4-(Morpholinomethyl Carbamoyl Phenyl) Furan-2-Carboxamide for brass in HCl medium. *Arabian J. Chem.* 2016; **9**, 121-35.
[24] D Njobuenwu, EO Oboho and RH Gumus. Determination of contact angle from contact area of liquid droplet spreading on solid substrate. *Leonardo Electron. J. Pract. Tech.* 2007; **6**, 29-38.
[25] BP Binks, L Isa and AT Tyowua. Direct measurement of contact angles of silica particles in relation to double inversion of pickering emulsions. *Langmuir* 2013; **29**, 4923-7.
[26] F Deng, L Wang, Y Zhou, X Gong, X Zhao, T Hu and C Wu. Effect of nanosilica content on the corrosion inhibition of composite coatings of a filled epoxy resin grafted with a hydrophobic fluoroalkylsilane: A dual critical concentrations interpretation. *RSC Adv.* 2017; **7**, 48876-93.
[27] HX Nguyen, NTT Dao, HTT Nguyen and AQT Le. Nanosilica synthesis from rice husk and application for soaking seeds. *IOP Conf. Ser. Earth Environ. Sci.* 2019; **266**, 12007.
[28] S Mirmohamadsadeghi and K Karimi. *Recovery of silica from rice straw and husk*. Elsevier, Amsterdam, 2020, p. 411-33.
[29] R Maddalena, C Hall and A Hamilton. Effect of silica particle size on the formation of calcium silicate hydrate [C-S-H] using thermal analysis. *Thermochim. Acta* 2019; **672**, 142-9.
[30] R Sekifuji and M Tateda. Study of the feasibility of a rice husk recycling scheme in Japan to produce silica fertilizer for rice plants. *Sustain. Environ. Res.* 2019; **29**, 11.
[31] SN Ishmah, MD Permana, ML Firdaus and DR Eddy. Extraction of silica from bengkulu beach sand using alkali fusion method. *PENDIPA J. Sci. Educ.* 2020; **4**, 1-5.

[32] LK Sakti, GAN Sheha, CPSM Radhiyah, J Nugraha, DR Eddy, MD Permana, IP Maksum and Y Deawati. Cotton fabric coating by rGO and polymethylsiloxane layer with antibacterial, hydrophobic and photothermal properties. *Trends Sci.* 2023; **20**, 6813.
[33] PH Chen, CC Hsu, PS Lee and CS Lin. Fabrication of semi-transparent super-hydrophobic surface based on silica hierarchical structures. *J. Mech. Sci. Tech.* 2011; **25**, 43-7.
[34] S Gharazi, A Ershad-Langroudi and A Rahimi. The influence of silica synthesis on the morphology of hydrophilic nanocomposite coating. *Sci. Iranica* 2011; **18**, 785-9.
[35] MA Shirgholami, MS Khalil-Abad, R Khajavi and ME Yazdanshenas. Fabrication of superhydrophobic polymethylsilsesquioxane nanostructures on cotton textiles by a solution-immersion process. *J. Colloid Interface Sci.* 2011; **359**, 530-5.
[36] U Kalapathy, A Proctor and J Shultz. A simple method for production of pure silica from rice hull ash. *Bioresource Tech.* 2000; **73**, 257-62.
[37] TS Hamidon, NA Ishak and MH Hussin. Enhanced corrosion inhibition of low carbon steel in aqueous sodium chloride employing sol-gel-based hybrid silanol coatings. *J. Sol Gel Sci. Tech.* 2021; **97**, 556-71.
[38] R Farid, K Rajan and DK Sarkar. Enhanced corrosion protection of aluminum by ultrasonically dip coated sodium silicate thin films. *Surf. Coating. Tech.* 2019; **374**, 355-61.